ACCOUNTS of chemical research

Article

pubs.acs.org/accounts

Developing DNA Nanotechnology Using Single-Molecule Fluorescence

Roman Tsukanov,[†] Toma E. Tomov,[†] Miran Liber, Yaron Berger, and Eyal Nir*

Department of Chemistry and the Ilse Katz Institute for Nanoscale Science and Technology, Ben-Gurion University of the Negev, Beer Sheva, 84105, Israel

CONSPECTUS: An important effort in the DNA nanotechnology field is focused on the rational design and manufacture of molecular structures and dynamic devices made of DNA. As is the case for other technologies that deal with manipulation of matter, rational development requires high quality and informative feedback on the building blocks and final products. For DNA nanotechnology such feedback is typically provided by gel electrophoresis, atomic force microscopy (AFM), and transmission electron microscopy (TEM). These analytical tools provide excellent structural information; however, usually they do not provide high-resolution dynamic information. For the development of DNA-made dynamic devices such as machines, motors, robots, and computers this constitutes a major problem. Bulk-fluorescence techniques are capable of providing dynamic information, but because only ensemble averaged information is obtained, the technique may not adequately describe the dynamics in the context of complex DNA devices. The single-molecule fluorescence (SMF) technique offers a unique combination of capabilities that make it an excellent tool for guiding the development of DNA-made devices. The technique has been increasingly used in DNA nanotechnology, especially for the analysis of structure, dynamics, integrity, and operation of DNA-made devices; however, its capabilities are not yet sufficiently familiar to the community. The purpose of this Account is to demonstrate how different SMF tools can be utilized for the development of DNA devices and for structural dynamic investigation of biomolecules in general and DNA molecules in particular. Single-molecule diffusion-based Förster resonance energy transfer and alternating laser excitation (sm-FRET/ALEX) and immobilization-based total internal reflection fluorescence (TIRF) techniques are briefly described and demonstrated. To illustrate the many applications of SMF to DNA nanotechnology, examples of SMF studies of DNA hairpins and Holliday junctions and of the interactions of DNA strands with DNA origami and origami-related devices such as a DNA bipedal motor are provided. These examples demonstrate how SMF can be utilized for measurement of distances and conformational distributions and equilibrium and nonequilibrium kinetics, to monitor structural integrity and operation of DNA devices, and for isolation and investigation of minor subpopulations including malfunctioning and nonreactive devices. Utilization of a flow-cell to achieve measurements of dynamics with increased time resolution and for convenient and efficient operation of DNA devices is discussed briefly. We conclude by summarizing the various benefits provided by SMF for the development of DNA nanotechnology and suggest that the method can significantly assist in the design and manufacture and evaluation of operation of DNA devices.

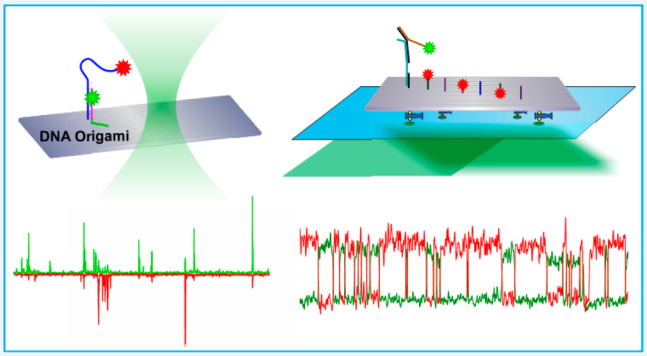

INTRODUCTION

Individual molecules are typically too small to be directly observed using visible light, a fact that has significantly hampered studies of biomolecules and efforts to rationally manipulate molecules into designed structures. Progress in these fields of research is, therefore, strongly dependent on the ability of analytical techniques to provide various, but partial, solutions for this major problem. This is also true in DNA nanotechnology: significant effort is invested in the analysis of the building blocks and final products of DNA-based structures and devices, yet the obtained information is limited.

The main analytical tools used in the field of DNA nanotechnology are gel electrophoresis, atomic force microscopy (AFM), and transmission electron microscopy (TEM and Cryo-EM). Gel electrophoresis, the main tool used in the early days of DNA nanotechnology,[1] is excellent for determining the size of a DNA construct and can provide useful information on structural integrity and stability of a DNA construct, and these abilities can be extended further using fluorescence and radioactive labeling.[2] AFM[3,4] and TEM[5−8] provide excellent two-[3] and three-dimensional[5−8] structural information and are frequently used for analysis of large DNA structures including DNA origami. DNA origami is usually made of a long DNA strand scaffold and many short DNA strands called staples that self-assemble into two[3] or three[5] dimensional, defined structures. In addition, recent advances in high-speed AFM (HS-AFM) technology enable acquisition of impressive dynamic information

Special Issue: Nucleic Acid Nanotechnology

Received: January 21, 2014
Published: May 14, 2014

   dx.doi.org/10.1021/ar500027d | Acc. Chem. Res. 2014, 47, 1789−1798

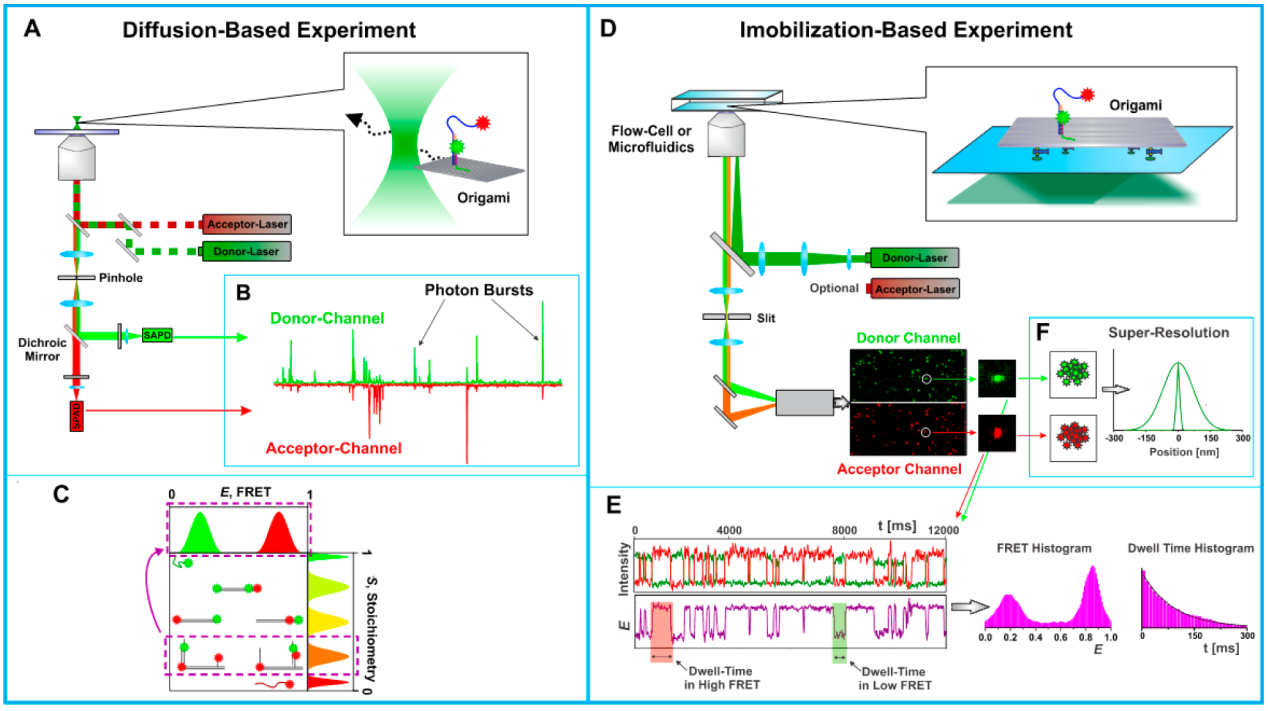

Figure 1. Single-molecule fluorescence diffusion-based sm-FRET/ALEX and immobilization-based sm-FRET/TIRF techniques. (A) Optical setup for diffusion-based experiment. (B) Typical time trajectory and photon bursts. (C) *E*/*S* histogram. (D) Optical setup for immobilization-based experiment. (E) Donor and acceptor intensities and *E* time trajectories of individual molecules and typical *E* histogram and dwell-time histogram calculated from the time trajectories. (F) The position of individual spots can be determined to achieve super-resolution microcopy.

in the preferable aqueous environment.[9,10] These analytical tools, however, are not *in situ* techniques, in that samples are usually not investigated in the aqueous environment or under conditions in which DNA structures are functional, resulting in two main disadvantages. First, the sample may be damaged during the switch to the measurement environment (gel medium or AFM or TEM surfaces). Second, with the exclusion of HS-AFM, it is difficult and sometimes impossible to measure dynamics with these techniques.

Fluorescence-based techniques are the methods of choice for *in situ* study of conformational dynamics of molecules, and bulk fluorescence was the main tool with which dynamics of DNA devices were studied until recently.[8,10−15] Because bulk fluorescence provides only averaged information, however, it often fails to capture the real complexity of a device. Valuable information regarding nonreactive and malfunctioning devices and about side products or any other minute population is often lost in the ensemble. These disadvantages are a major problem for the development of dynamic DNA devices.

The single-molecule fluorescence (SMF) approach overcomes these limitations. Structural dynamics and interaction information on DNA, RNA, proteins, and DNA−protein complexes[16,17] can be obtained with the SMF technique, and it has increasingly become a leading tool in DNA nanotechnology.[18−36] The approach, which draws on different methods,[37−42] offers a unique combination of features that enables molecular analysis beyond what is possible with more classical methods, thereby expanding the toolkit available for developing DNA-based devices and particularly for the study of their dynamics.

The noninvasive character of the fluorescence method enables *in situ* measurements and allows the system to be maintained in the favored aqueous environment. Single-molecule Förster resonance energy transfer (FRET) provides subnanometer structural information not available through any other method. When coupled to alternating laser excitation (sm-FRET/ALEX),[43−45] the technique provides stoichiometric information, allowing determination of the presence or absence of building blocks and device integrity. In addition, in cases in which a molecule fluctuates between states, observation of individual molecules may yield kinetic information without a need for nonequilibrium conditions (initiation of kinetic experiment). The single-molecule immobilization-based total internal reflection (TIRF) technique[39,41,46] enables continuous observation of individual molecules and, in conjunction with a flow-cell, enables fast replacement of the surrounding solution to facilitate kinetic measurements and convenient introduction of building blocks and removal of waste products of the operation of DNA machines. Finally, because measurements are conducted on individual molecules, the information acquired reflects the distribution of properties rather than the average, enabling detection of minute populations and identification of side products and malfunctioning and nonreactive devices.[18,24,25,28] This ability is significantly strengthened using the ALEX technique, which enables isolation and sorting of subpopulations of interest out of the ensemble, increasing resolution.[18,19,23−27]

This Account is organized as follows: Diffusion-based sm-FRET/ALEX and immobilization-based TIRF techniques are briefly explained, and the benefits of each technique and which is preferred for what purpose are discussed. sm-FRET/ALEX is then explained in more detail, and various diffusion-based studies are presented. This is followed by a detailed explanation of the TIRF technique and presentation of various immobilization-based studies. For reasons of clarity, examples of SMF studies of relatively simple systems, such as DNA hairpins[26,27] and Holliday junctions,[20] are provided first, followed by introduction of more complex DNA origami[30,31] and DNA bipedal motor[25] systems. Because the aim of this Account is to demonstrate advantages of

dx.doi.org/10.1021/ar500027d | *Acc. Chem. Res.* 2014, 47, 1789−1798

SMF to the DNA nanotechnology field and to introduce recent advances, we have not attempted to review all studies that employ SMF, especially those reviewed[47−52] before. Super-resolution microscopy studies[28,29,31,36] are only briefly discussed.[30]

ADVANTAGES AND DISADVANTAGES OF DIFFUSION-BASED AND IMMOBILIZATION-BASED METHODS

Generally, in SMF experiments samples either diffuse freely in the solution or are immobilized on the coverslip surface; examples of both are discussed in the following sections. In the former, picomolar concentrations of fluorescently labeled molecules (or complexes of molecules) diffuse in and out of the confocal spot providing bursts of photons that are usually collected using high time-resolution single-photon avalanche diode (SPAD, ∼200 ps). As a result, the method provides high-resolution snapshots of the state of individual molecules. In the immobilization-based technique, individual molecules are continuously observed using an EMCCD camera; these experiments have lower time-resolution than that of the SPAD (∼1−10 ms) but provide time evolution information (essentially a "movie") of individual molecules.

Diffusion-based (Figure 1A) and immobilization-based (Figure 1B) approaches carry advantages and disadvantages, and each is more suitable to answer certain types of questions. Because the diffusion-based method does not require sample immobilization, difficulties associated with the immobilization process and chemistry and due to possible interactions with the coverslip surface are avoided, and therefore, the experiments are usually faster and easier to conduct. The sample molecules are replaced continually by diffusion, and by use of reducing/oxidizing systems (e.g., Trolox[53]) and bright and photostable fluorophores (e.g., CY3B, ATTO-532, ATTO-550, ATTO-647N), photobleaching and blinking can be almost completely avoided (Figure 2A), significantly reducing experimental artifacts.

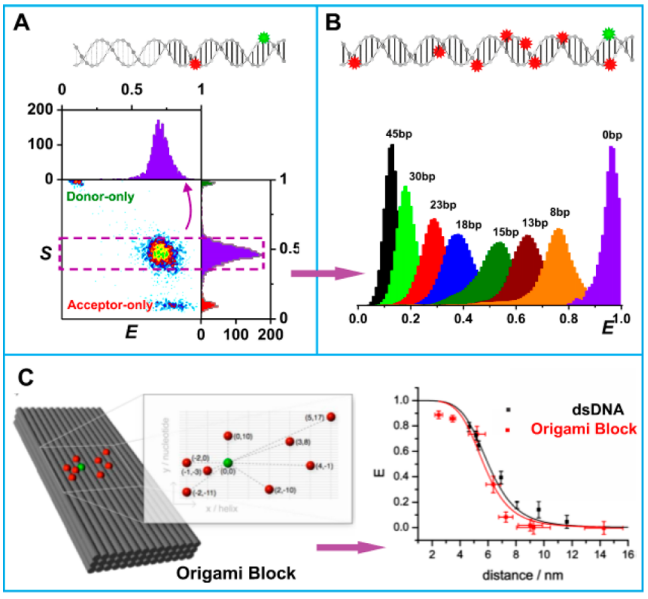

Figure 2. Obtaining distances in diffusion-based sm-FRET/ALEX. (A) E/S-histogram of donor and acceptor labeled double-stranded DNA. (B) Overlay of eight E histograms of double-stranded DNA labeled with donor and acceptor at different base pair (bp) distances. (C) Origami serves as a distance ruler for FRET measurements. Adapted from ref 21.

The continuous observation of individual molecules allowed by the immobilization-based method enables direct observation of conformational changes and of interactions with molecules freely diffusing in the solution, from which transition rates and association and dissociation rates can be obtained. Based on intensity and the number of bleaching steps, immobilization enables better assessment of the number of fluorophores present on an individual molecular unit than does a diffusion-based experiment. Moreover, the ability of TIRF to reject background emission enables affinity measurement in higher concentration than possible in diffusion-based experiments. Furthermore, by using a flow-cell,[38,39] the surrounding solution can be replaced while the sample molecule remains in position and is continuously observed. This is a significant advantage because it enables introduction of various components (e.g., building blocks, DNA fuels, see definition below) and removal of leftovers and waste without the need to transfer the sample to a different environment (e.g., using gel electrophoresis or other filters). Finally, super-resolution microscopy is possible only for immobilized samples.[28−31]

DIFFUSION-BASED sm-FRET/ALEX: THE TECHNIQUE

With the ALEX technique[43,44] (also called PIE[45]), two or more lasers,[22] each directly exciting a corresponding fluorophore, alternate (Figure 1A). Each burst of photons (Figure 1B) produced during the transit of an individual molecule through the confocal spot (the 3D volume in which molecules are observed, roughly 0.3 μm across and 1.5 μm in length) is analyzed in terms of the FRET efficiency and fluorophore stoichiometry (E and S, respectively). The FRET efficiency, defined as $E = A_{D_{EX}}/(D_{D_{EX}} + A_{D_{EX}})$, where $D_{D_{EX}}$ and $A_{D_{EX}}$ are the number of donor and the acceptor photons, respectively, recorded during the time the donor laser is on, reflects the donor−acceptor distance. The stoichiometry ratio, defined as $S = D_{EX}/(D_{EX} + A_{EX})$, where D_{EX} and A_{EX} are the sums of the numbers of donor and acceptor photons recorded during the times the donor laser and the acceptor laser are on, respectively, reflects the fluorophore stoichiometry independently of the E value. The results are placed in a two-dimensional E/S histogram that reports on the distributions of donor/acceptor stoichiometry and donor−acceptor distances in the different sample molecules present in the solution (Figure 1C). Other properties of the burst, such as the total number of photons and the duration, are also calculated and provide information on the size of the molecule and the total number of fluorophores attached to the molecule. The method has been used in a number of DNA nanotechnology studies.[18−27]

DIFFUSION-BASED sm-FRET/ALEX: BASIC EXAMPLES

Sorting and Detecting Minute Populations

A two-dimensional E/S-histogram of a duplex DNA made of donor and acceptor labeled strands is presented in Figure 2A. The S values of the doubly labeled duplex are centered on 0.5 indicting the presence of an equal number of donors and acceptors (in fact, one of each fluorophore). Small amounts of donor-only and acceptor-only populations are observed in S = 0.1 and S = 1, respectively. The E-histogram projections are constructed only from events that have S values around 0.5 (Figure 2A, purple rectangle), rejecting events in which one of the fluorophores is absent or not fluorescently active. This example demonstrates that the ALEX technique is capable of identifying and separately investigating different populations including those that account for only a fraction of the total (<1%).

dx.doi.org/10.1021/ar500027d | Acc. Chem. Res. 2014, 47, 1789−1798

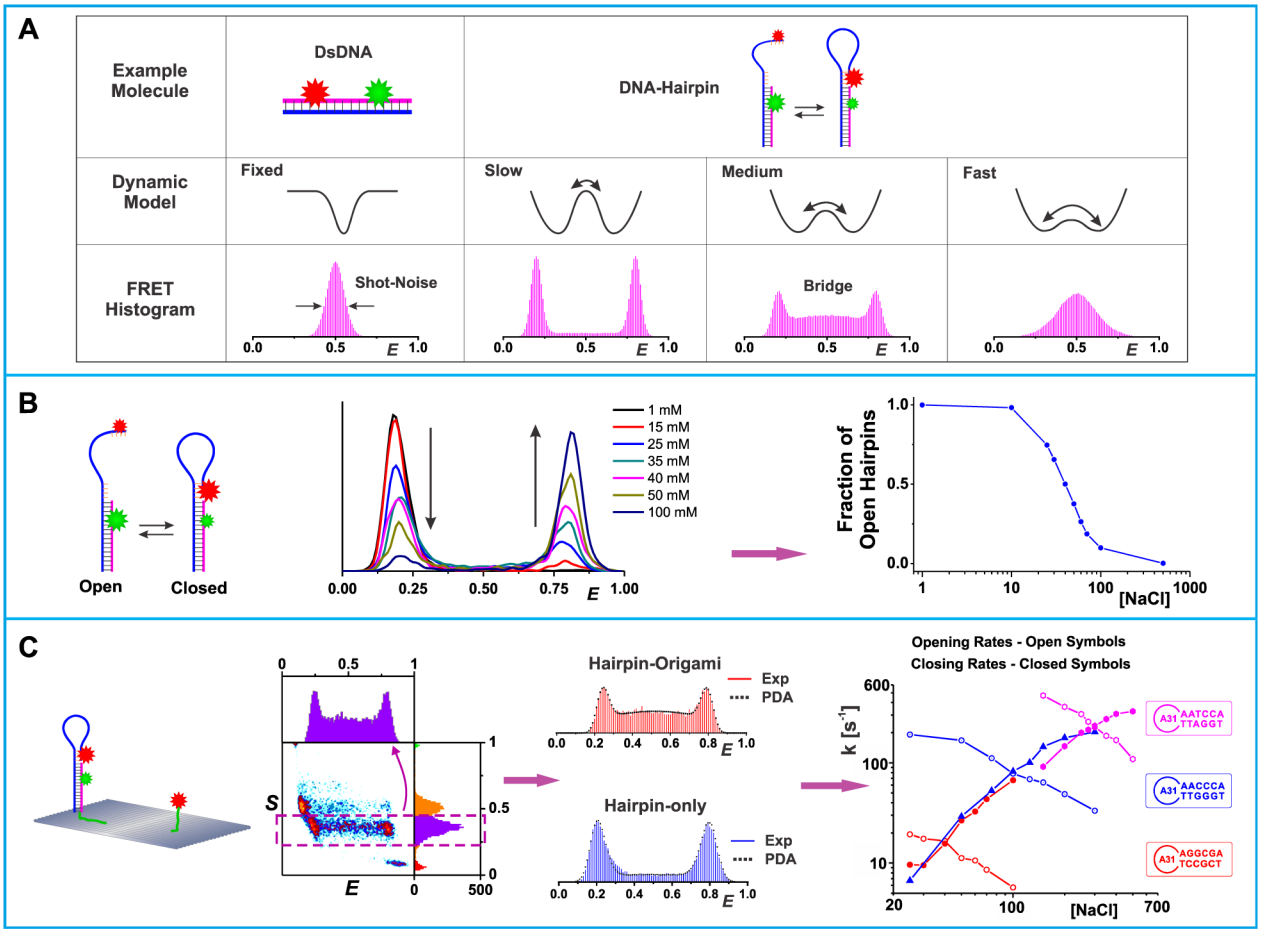

Figure 3. Obtaining dynamics in diffusion-based sm-FRET/ALEX. (A) Schematic of the influence of dynamics on the shape of *E* histograms. Adapted from ref 27. (B) Schematic of the hairpin-only *E* histograms measured at various NaCl concentrations and plot of fraction of open state. Adapted from ref 26. (C) Schematic of hairpin attached to origami, *E*/*S*-histogram of hairpin−origami, *E* histograms of hairpin−origami and identical hairpin-only, and summary of the opening and closing rates of hairpins with poly(A_{31}) loop and different stems (chevron plot). Adapted from ref 27.

Donor−Acceptor Distance and Förster Radius

The energy transfer between donor and acceptor is dependent on, among other factors, the donor−acceptor distance.[37] For commonly used fluorophores, FRET is sensitive to distances from 1 to 10 nm, corresponding to a DNA duplex length of up to 35 base pairs as shown in Figure 2B. Stein et al.[21] showed that using rigid origami blocks and several pairs of donor and acceptor fluorophores placed on the same side of the origami at various distances apart, it was possible to determine the Förster radius (R_0) of the pair with good accuracy and without using multi-parametric fitting as required for commonly used double-stranded DNA (Figure 2C).

Obtaining Dynamic Information

The shape of an *E*-histogram reflects the conformational dynamics of a molecule (Figure 3A),[44] and analysis of the histogram shape using probability distribution analysis (PDA)[44,54,55] provides information on molecular dynamics. For a fixed donor−acceptor distance, the histogram contains only a single peak with width dependent on photon statistics (shot noise[44,56]). In case of a molecule that interconverts between two states with rates much slower than the diffusion time, two peaks are observed in the histogram.[27] A molecule that interconverts between the states during the burst yields *E* values that are average of the *E* values of the states (weighted by the time the molecule spent in each state, called a bridge). The probability for detecting transition events increases with an increase in transition rates and also increases with an increase in the time the molecule spends in the confocal spot. Figure 3B shows the *E* histograms of a two-state DNA hairpin measured in different NaCl concentrations.[26] The absence of intermediate *E* values (i.e., a bridge) in the histograms indicates that the opening and closing rates are much slower than the burst duration and indicate the absence of a stable intermediate state, following a two-state model. The hairpin stability is depended on NaCl concentration, as is reflected in the fraction of open hairpins. Hairpins can be attached to origami to slow the diffusion and by that increase the probability to observe transitions (Figure 3C). To distinguish between hairpin−origami and hairpin-only (residuals from the annealing), the origami was labeled with an additional acceptor, and the *E* histograms were constructed only from events with the corresponding *S* values (bursts inside the purple rectangle, Figure 3C). Because of its slower diffusion, the hairpin−origami *E* histogram has a larger bridge than that of the identical free hairpin. Figure 3C shows how the closing rates of a series of three hairpins differing only in stem sequences (all have polyA_{31} loops) depend on the NaCl concentration but not on the stem sequence. In contrast, the opening rates, which depend on the thermodynamic stability of the stem, are dependent on the stem sequence and on the salt concentration.[27]

dx.doi.org/10.1021/ar500027d | *Acc. Chem. Res.* 2014, 47, 1789−1798

sm-FRET/ALEX: APPLICATIONS IN DNA NANOTECHNOLOGY

Verifying the Presence of Staples

Figure 4A shows the E/S histograms of origami containing two elongated staples (staples are short stands that construct the origami[3]) that are labeled with green and red fluorophores. The S histogram shows that at least 97% of the origami are doubly labeled, verifying that less than 3% of the staples are missing.

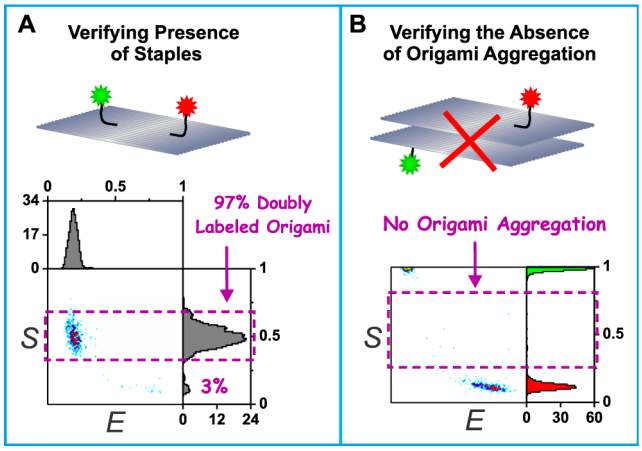

Figure 4. Examples of the use of sm-FRET/ALEX in DNA nanotechnology: (A) verification of the presence of staples on DNA origami; (B) verification of the absence of origami aggregates.

Verifying the Absence of Origami Aggregation

To verify the absence of origami aggregation, the origami strands were annealed in the presence of a mixture of staples labeled with green or red fluorophores (Figure 4B). Each origami should be decorated, therefore, by either a single green or a single red fluorophore, and the absence of intermediate S values indicates absence of aggregates. To reduce aggregation, the origami was treated for 10 min in a salt free buffer (1× TAE) before the measurement,[26] and its structural integrity was verified using AFM (data not shown). Without this treatment, 5−10% intermediate S values are usually observed (data not shown).

Monitoring Device Operation

Tomov et al.[25] demonstrated how the SMF technique can monitor the progress of a nonautonomous bipedal walker,[12] report operational yields, and identify unreactive motors and operational errors (Figure 5). In this device, a walker strides on an origami track powered by sequential interactions with externally introduced fuel (F) and antifuel (AF) DNA strands. Fuel is a DNA strand that can connect and bridge two other strands (the leg and the foothold in this case, Figure 5A), and antifuel is a complementary strand that can connect to the fuel to release the leg and the foothold.[12,25] In the initial state, 98% of the motors consist of a walker and an origami track (S = 0.25). Only 2% of the origami (acceptor only population, S = 0.1) do not contain a walker (Figure 5B). Most of the motors show low E values as expected for the initial state in which the donor-labeled leg is lifted. Upon fuel addition, 96% of the motors react properly in the first step (Figure 5C). Unreactive motors make up 26% of the population after five sequential steps (Figure 5D). As is evident by the presence of two peaks in step 4, some of the motors (36%) step backward instead of forward. This happens because footholds 1 and 5 are identical and because of the short

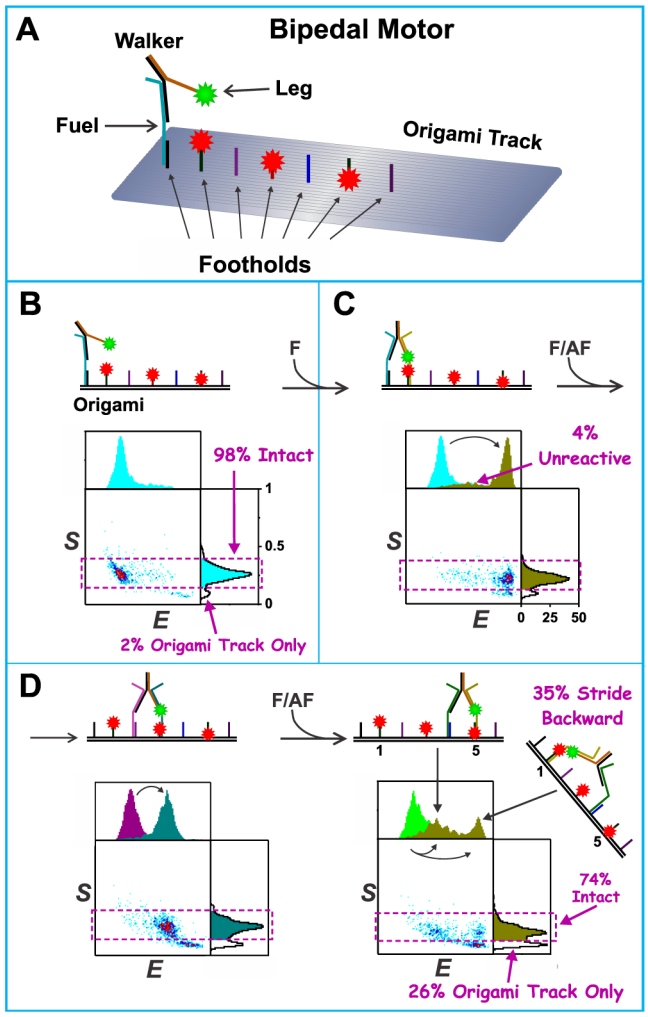

Figure 5. Use of sm-FRET/ALEX in DNA nanotechnology is demonstrated by the analysis of a bipedal motor striding on origami track. Adapted from ref 25. (A) Schematic of the bipedal motor. (B) Monitoring of the initial state; 98% of the tracks consist of a bipedal walker. (C) Monitoring of progress; 4% of the motors did not react properly. (D) In this example, 26% of the tracks lost the walker and 35% of the walkers stepped backward.

distance between the track footholds (6.5 nm). A similar motor with twice the distance between the footholds strides only in the desired direction (data not shown). In an earlier work, Masoud et al.[24] used SMF to monitor the assembly and operation (yield and kinetics) of autonomous bipedal walker.[2]

Analyzing Mechanisms Involved in the Operation of Bipedal Motor Leads to Rational Design

SMF enables analysis of the mechanisms of DNA reactions including those occurring in the context of complex devices. Figure 6 shows how sm-FRET/ALEX was used to reveal the mechanism of leg-lifting and leg-placing reactions in a bipedal walker that eventually led to the rational design of improved fuels.[25] The reaction kinetic profiles were obtained by monitoring the changes in leg-lifted and leg-placed populations (low and high E values, respectively) upon introduction of fuels and antifuels (Figure 6A). Analysis of the kinetic profiles of the leg-lifting reaction (Figure 6B) indicates that given enough antifuels and incubation time, 100% of the legs are lifted from the foothold, indicating that the leg-lifting reaction is not the reason for the incomplete operation of the motor observed in Figure 5D.[25]

dx.doi.org/10.1021/ar500027d | Acc. Chem. Res. 2014, 47, 1789−1798

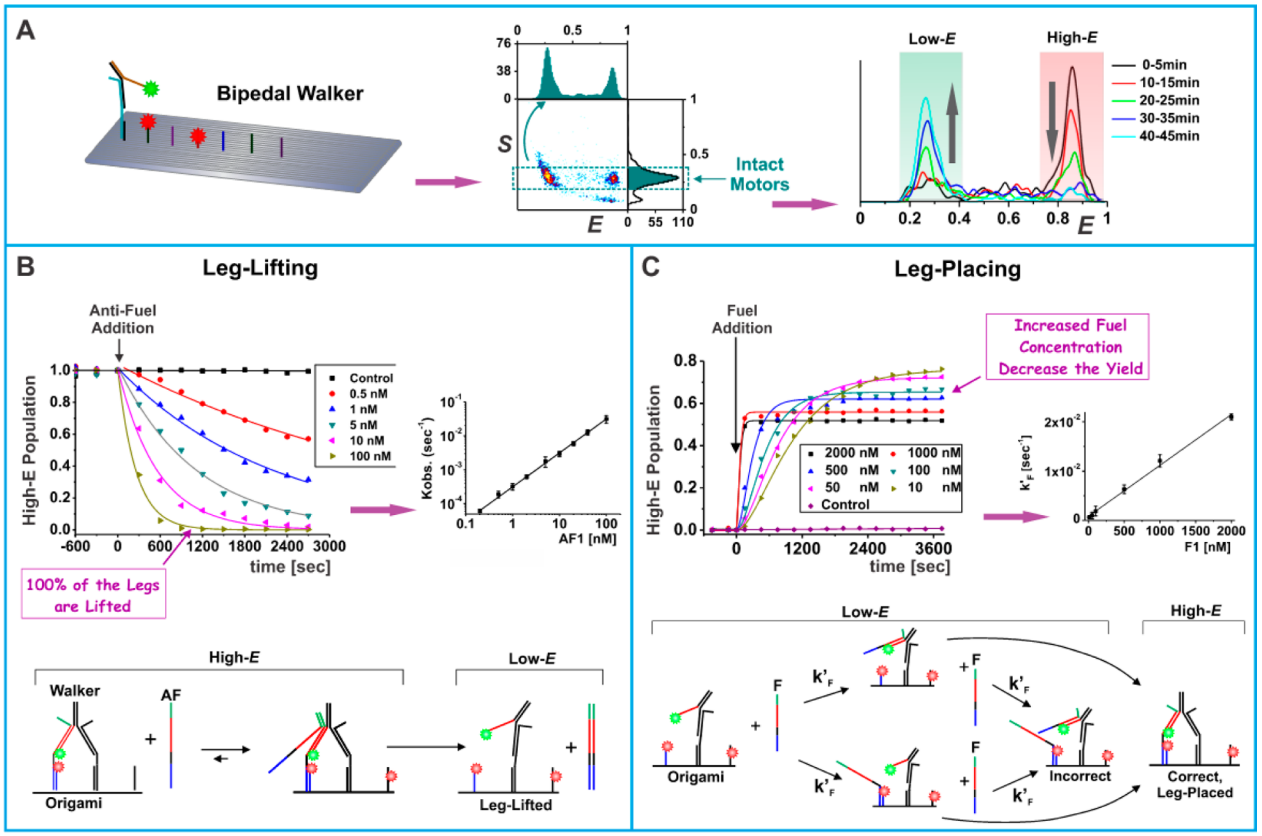

Figure 6. Resolving the operation mechanism of bipedal walker by sm-FRET/ALEX analysis of reaction kinetics. Adapted from ref 25. (A) Schematic of sm-FRET/ALEX method for obtaining kinetic profiles. The fraction of high and low *E* populations changes with time as indicated by the change in the *E* histograms. Kinetic profiles are calculated from these histograms. (B) Kinetic profiles, obtained rates, and proposed reaction diagram of leg-lifting reaction. (C) Kinetic profiles, obtained rates, and proposed reaction diagram of leg-placing reactions.

Analysis of the kinetic profiles of the leg-placing reaction indicates that increased fuel concentration results in lower reaction yield, most likely because of binding of fuels to the foothold and to the leg that prevents leg placing (Figure 6C, the incorrect structure in the reaction diagram). This problem was solved by using fuels that form hairpins. This dictates that the fuel binds first to the footholds and then, upon hairpin opening, to the leg (data not shown).[25] This example demonstrates that the SMF can provide very useful kinetic information that reveals problems with design, in this case, the simultaneous binding of fuels to leg and foothold. SMF thus enables rational design of improved devices.

IMMOBILIZATION-BASED TIRF: THE TECHNIQUE

Complementary to the diffusion-based technique is the immobilization-based technique in which the sample molecules are immobilized on a coverslip surface (often using biotin−avidin interaction). Immobilization has also been used in analysis of DNA devices.[28−36] Alternative approaches, such as prism-type TIRF[39,41] or detection using SPAD[57] instead of a camera (which requires scanning confocal microscopy), are also available. In the objective-type TIRF technique (Figure 1D), one or more lasers are focused on the side of the back focal plane of a high-NA oil objective, and because of the high incident angle with which the light hits the coverslip−solution interface, an evanescent light is created. This reduces the amount of background light coming from fluorescent species that may be present in the solution. The photons emitted from the individual sample molecules are collected by the same objective and, after separation based on wavelength, are imaged on an EMCCD camera. Each individual spot in the image corresponds to an individual molecule. The data collected by the camera can be analyzed in several ways. In the case of FRET measurement, the intensity of the individual donor and acceptor spots are measured over time and the FRET value is calculated for each time bin (called the time trajectories, Figure 1E). The time trajectories can be analyzed in terms of the FRET value distributions and the time duration that the molecule spends in each state (dwell times) from which the rate of transition between states can be calculated. Immobilization is also crucial for super-resolution microscopy, in which the positions of individual emitters can be determined with resolution down to several nanometers (Figure 1F). The technique enables tracking particles over long distances (for example, of a DNA motor striding on origami[28]), measurement of the distance between two fluorophores attached to origami (beyond the ∼10 nm possible using FRET[29]), and imaging of nanoscale topography and measurements of binding/unbinding rates using point accumulation for imaging in nanoscale topography (PAINT) method,[30,31] and thus it is expected to take an increased role in DNA nanotechnology.

IMMOBILIZATION-BASED TIRF: DNA DYNAMICS AND APPLICATION IN DNA NANOTECHNOLOGY

Measuring Dynamics of DNA Hairpins and Holliday Junctions

Using the immobilization-based method, Tsukanov et al.[26] have measured the fraction of open state and the opening and closing rates of DNA hairpins (Figure 7A) that were either directly

dx.doi.org/10.1021/ar500027d | Acc. Chem. Res. 2014, 47, 1789−1798

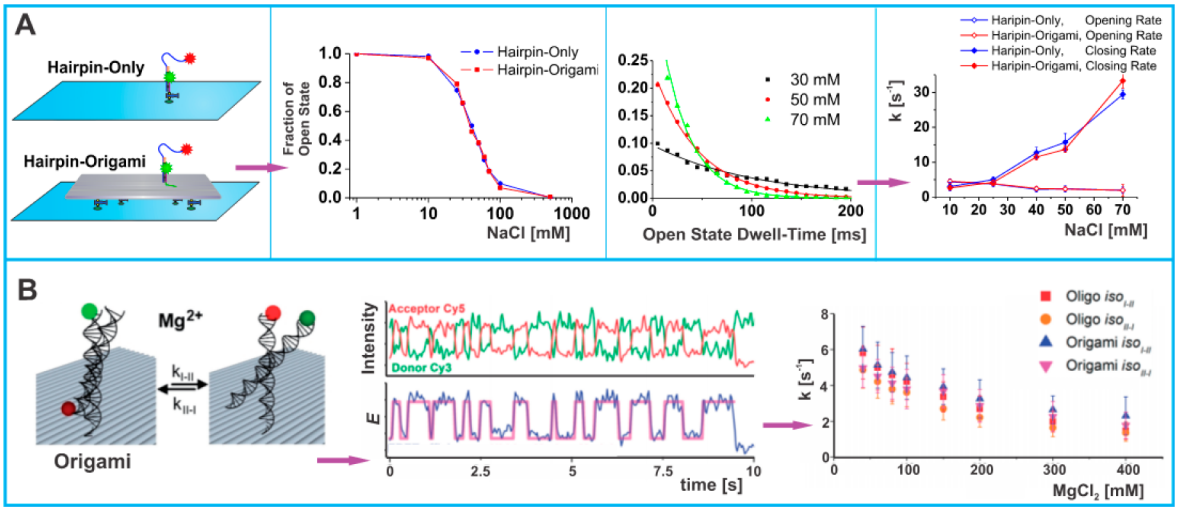

Figure 7. Examples of immobilization-based sm-FRET/TIRF for DNA dynamic studies using origami. (A) Fraction of open state, dwell-time histograms, and opening and closing rates of immobilized hairpin (hairpin-only) and hairpin attached to immobilized origami (hairpin−origami). Adapted from ref 26. (B) Directly immobilized Holliday junctions and Holliday junctions attached to immobilized origami, time trajectories, and the obtained rates. Adapted from ref 20.

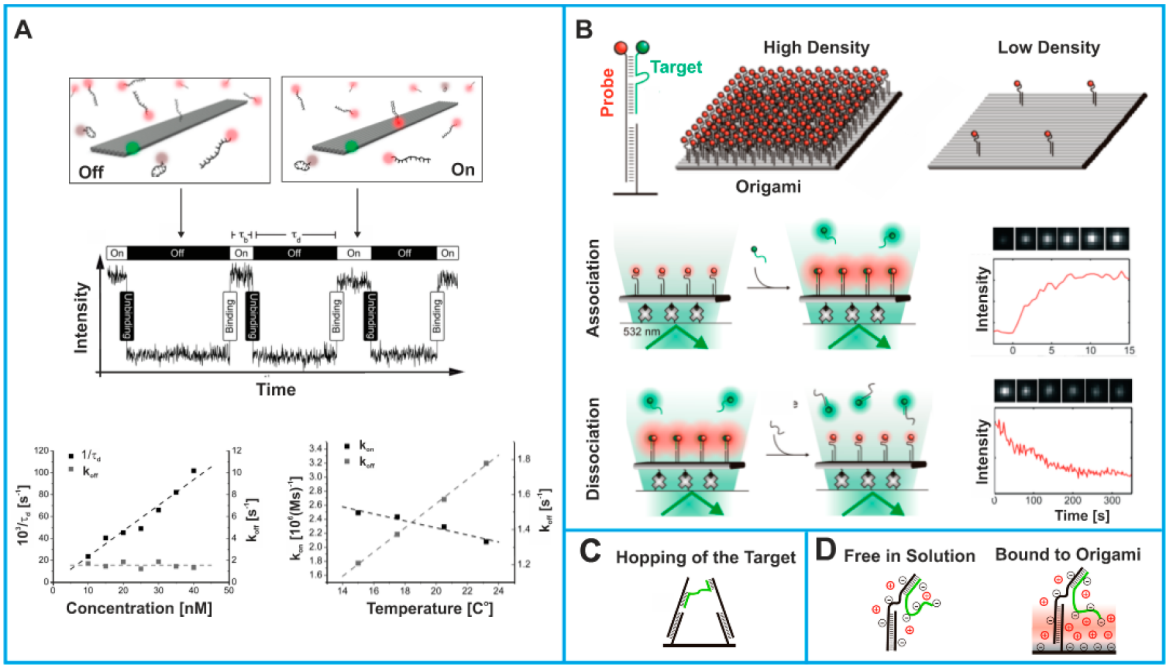

Figure 8. Examples of immobilization-based sm-FRET/TIRF using origami for study of DNA dynamics. (A) Association and dissociation rates of freely diffusing strands to strands attached to origami were directly determined for different strand concentrations and temperatures. Adapted from ref 30. (B) Association and dissociation rates of freely diffusing strands to and from different densities of strands attached to origami were directly determined. Adapted from ref 33. (C) Proposed mechanism for hopping. (D) Proposed mechanism for cation requirement that slows dissociation.

immobilized on a coverslip surface (through a biotin−avidin interaction) or attached to origami that was immobilized on the surface (also using biotin−avidin binding).[26] The data show that there are no differences in the stability or kinetics of the two constructs. The opening and the closing rates are in good agreement with rates obtained using diffusion-based PDA[27] (as in Figure 3C). In an earlier study, Gietl et al.[20] showed that the dynamics of an immobilized Holliday junction are identical to that of a Holliday junction attached to surface-immobilized origami (Figure 7B). These two studies support the biocompatibility[20] of DNA origami.

Determining Association and Dissociation Rates

Using DNA-PAINT, Jungmann et al.[30] determined the association and dissociation rates of a fluorescently labeled freely diffusing DNA strand to a complementary sequence attached to an immobilized origami (Figure 8A). This was achieved by observing the fluorescence on- and off-times and demonstrated that kinetics can be measured even without FRET. They determined the dependencies of the association and dissociation rates on strand concentration and on temperature. The concentration of the freely diffusing fluorescently labeled strands was as high as 40 nM, producing high background signal. Due to the use of the TIRF method, however, the signal that

dx.doi.org/10.1021/ar500027d | Acc. Chem. Res. 2014, 47, 1789−1798

originated from the hybridized strand was stronger than the background (which can be high in PAINT experiments). Johnson-Buck et al.[33] used FRET to study the dependency of association and dissociation rates of a donor-labeled DNA strand to and from a complementary acceptor-labeled probe arranged on an immobilized origami as a function of the probe density (Figure 8B). The dissociation rates were up to an order of magnitude slower in the dense probe arrangement than for single probes, and the binding rates were also reduced, although not as much. The slowed dissociation rates were explained by hopping of the target strand between adjacent probe strands (Figure 8C). This study also showed that, even in the absence of hopping, the dissociation rate (and, to lesser extent, the association rate) may be influence by the presence of the origami, possibly because the negatively charged origami recruits cations that screen the negative charge more than are recruited in the absence of origami. The hairpin[26] and the Holliday junction[20] dynamics were not influenced by the origami, whereas the dissociation and association of target DNA (especially of long strands) were somewhat influenced, indicating that the biocompatibility of the origami may be system dependent. In a different study Scheible et al.[35] used lithography to create gold nanoislands on a glass coverslip on which rectangle origami were placed. They then used PAINT to image the islands, to characterize the origami occupancy of the islands, and to study the kinetics and efficiency of DNA strand displacement reaction. Lithography should enable the creation of organized DNA structures much larger than possible using only origami technology.

Measuring Fast Kinetics and Motor Operation Inside a Flow Cell

In the association−dissociation experiment mentioned above,[33] the reactions were initiated by exchange of buffer with or without the target strand. The fact that the origami was immobilized on the surface enabled buffer replacement and convenient initiation of the nonequilibrium kinetic measurement, demonstrating an important benefit of sample immobilization. Using a flow cell, we have measured the kinetics of leg lifting and leg placing of a bipedal motor with a time resolution faster than a second (Figure 9).

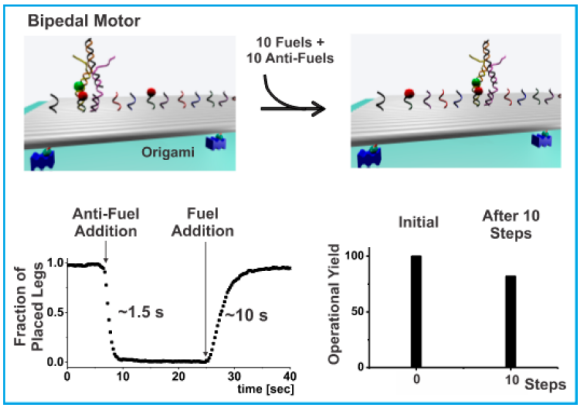

Figure 9. A bipedal motor operates inside a microfluidics device. Kinetic profiles of leg-lifting and leg-placing reactions and operational yield measured after 10 steps are presented.

The kinetic profiles demonstrate that DNA motors can react with rates that are as fast as a second. Furthermore, the flow cell enables removal of the excess fuels and antifuels resulting in improved yield relative to freely diffusing motors.

IMPLEMENTATION OF SMF IN DNA NANOTECHNOLOGY: A WORD OF CAUTION

For an SMF study to be successful many experimental issues need to be addressed properly. This includes, to name a few, fluorophore labeling and purification after labeling, sample immobilization, optical setup, data analysis, software, interpretation of the results, and treatment of artifacts (e.g., photobleaching and blinking and unwanted interaction with the coverslip surface), some of which are not trivial. The efforts required for initial successful SMF experiments for nonexperts may be an order of magnitude more than those required for initial successful AFM, TEM, or gel electrophoresis experiments, even when commercial optical setup is available. On the other side, once the many experimental issues are properly addressed and experience is gained, diffusion-based experiments may be simpler than AFM, TEM, and gel electrophoresis experiments, and immobilization-based experiments are comparable. These may explain why SMF has been adopted somewhat slowly in the DNA nanotechnology community. In order to save time and resources, we recommend considering collaboration with SMF experts who can better assess whether the questions asked can be addressed using SMF. Indeed, most of the SMF studies in the field of DNA nanotechnology have been carried out through such collaborations.

CONCLUDING REMARKS

The single-molecule fluorescence (SMF) technique offers a unique combination of capabilities that make it an excellent tool for assisting the development of DNA nanotechnology. As is evidenced by the various examples presented here, the technique is appropriate for detailed study of high temporal and spatial resolution dynamics and complicated interactions. SMF enables (i) elucidating the mechanisms involved in the operation of DNA devices, (ii) monitoring the structural integrity of DNA devices, (iii) studying the interaction of the device components, (iv) investigating minute populations, and (v) identifying malfunctioning and nonreactive devices and operational errors, all very beneficial for the development of dynamic devices.

SMF is not always the appropriate analytical tool. For imaging of two- and three-dimensional DNA structures with sizes larger than several nanometers, AFM and TEM are more suitable. Recent advances in super-resolution microscopy and the development of PAINT, however, enable single-molecule imaging over distances and resolution larger than several nanometers. These techniques have many of the advantages of SMF including the ability to investigate in the preferred aqueous environment. Gel electrophoresis is probably better for estimating the sizes of molecular structures, since a simple SMF method for size estimation is lacking. High-speed AFM may be preferable for imaging conformational changes, however, depending on the molecular system, AFM may have lower resolution and throughput than SMF.

To conclude, we believe that the SMF approach has the potential to significantly increase the quality and quantity of structural and dynamic information obtained for DNA devices, and this should enable more rational design, manufacture, and operation of increasingly better and more complex structures and devices made of DNA and other types of molecules. For example, continuous, *in situ* high-resolution monitoring and super-resolution imaging of the operation of a DNA machines that may manipulate guest molecules, possibly placed inside a microfluidics device and arranged into a large scale structure using lithography, should be possible in the near future. Finally,

we envision that a computer-controlled microfluidics flow cell, which enables sequential introduction and removal of building-blocks, will be used for the assembly of molecular structures that are impossible to assemble using conventional preparation methods; this use of microfluidics cells will be analogous to solid-phase synthesis.

AUTHOR INFORMATION

Corresponding Author

*E-mail: Eyalnir@Bgu.ac.il.

Author Contributions

†Roman Tsukanov and Toma E. Tomov have contributed equally to this work.

Notes

The authors declare no competing financial interest.

Biographies

Roman Tsukanov received his B.S. in physics in the Technion (Israel Institute of Technology), M.Sc. in physics at Ben-Gurion University of the Negev under the guidance of Prof. M. Feingold, and Ph.D. degree under the supervision of Dr. Nir. He developed and validated SMF techniques using DNA hairpins as model molecules and performed detailed investigation of DNA hairpin dynamics, assisted by DNA origami. He is also involved in developing microfluidics technology to operate DNA devices.

Toma E. Tomov received his B.S and M.Sc. degrees in chemistry from BGU. He is currently conducting his Ph.D. research with Dr. Nir. In his M.Sc. studies, he developed statistical algorithms for disentangling of subpopulations in single-molecule FRET/ALEX experiments. His current research interests are developing DNA motors using SMF techniques and microfluidics technology.

Yaron Berger received his B.S. degree in chemistry from BGU, and he is currently a M.Sc. student working with Dr. Nir. He is focusing on developing DNA motors with several pairs of legs to achieve increased operational yield.

Miran Liber received his B.S. degrees in chemistry and chemical engineering from BGU, and he is currently a Ph.D. student working with Dr. Nir. He specializes in developing DNA origami 3D frames for DNA motors, including micrometer-sized tracks, and is characterizing these using SMF and AFM and TEM techniques.

Eyal Nir is an assistant professor at the Chemistry Department in BGU and a member of the Ilse Katz Institute for Nanoscale Science and Technology. His Ph.D. studies with Prof. Mattanjah de Vries, at the Hebrew University, Jerusalem, were focused on gas-phase UV–IR spectroscopy of DNA building blocks. In his postdoctorate research at UCLA with Prof. Shimon Weiss, he developed the FRET/ALEX and PDA methods and studied DNA hairpin dynamics. His research group specializes in single-molecule fluorescence and applications to DNA nanotechnology and DNA and nucleosome dynamics.

REFERENCES

(1) Chen, J. H.; Seeman, N. C. Synthesis from DNA of a Molecule with the Connectivity of a Cube. *Nature* **1991**, *350*, 631–633.

(2) Omabegho, T.; Sha, R.; Seeman, N. C. A Bipedal DNA Brownian Motor with Coordinated Legs. *Science* **2009**, *324*, 67–71.

(3) Rothemund, P. W. K. Folding DNA to Create Nanoscale Shapes and Patterns. *Nature* **2006**, *440*, 297–302.

(4) Gu, H. Z.; Chao, J.; Xiao, S. J.; Seeman, N. C. A Proximity-Based Programmable DNA Nanoscale Assembly Line. *Nature* **2010**, *465*, 202–205.

(5) Douglas, S. M.; Dietz, H.; Liedl, T.; Hogberg, B.; Graf, F.; Shih, W. M. Self-Assembly of DNA into Nanoscale Three-Dimensional Shapes. *Nature* **2009**, *459*, 414–418.

(6) Bai, X. C.; Martin, T. G.; Scheres, S. H. W.; Dietz, H. Cryo-Em Structure of a 3d DNA-Origami Object. *Proc. Natl. Acad. Sci. U. S. A.* **2012**, *109*, 20012–20017.

(7) Liedl, T.; Hogberg, B.; Tytell, J.; Ingber, D. E.; Shih, W. M. Self-Assembly of Three-Dimensional Prestressed Tensegrity Structures from DNA. *Nat. Nanotechnol* **2010**, *5*, 520–524.

(8) Andersen, E. S.; Dong, M.; Nielsen, M. M.; Jahn, K.; Subramani, R.; Mamdouh, W.; Golas, M. M.; Sander, B.; Stark, H.; Oliveira, C. L. P.; Pedersen, J. S.; Birkedal, V.; Besenbacher, F.; Gothelf, K. V.; Kjems, J. Self-Assembly of a Nanoscale DNA Box with a Controllable Lid. *Nature* **2009**, *459*, 73–U75.

(9) Rajendran, A.; Endo, M.; Hidaka, K.; Sugiyama, H. Direct and Real-Time Observation of Rotary Movement of a DNA Nanomechanical Device. *J. Am. Chem. Soc.* **2013**, *135*, 1117–1123.

(10) Wickham, S. F.; Endo, M.; Katsuda, Y.; Hidaka, K.; Bath, J.; Sugiyama, H.; Turberfield, A. J. Direct Observation of Stepwise Movement of a Synthetic Molecular Transporter. *Nat. Nanotechnol.* **2011**, *6*, 166–169.

(11) Yurke, B.; Turberfield, A. J.; Mills, A. P.; Simmel, F. C.; Neumann, J. L. A DNA-Fuelled Molecular Machine Made of DNA. *Nature* **2000**, *406*, 605–608.

(12) Shin, J. S.; Pierce, N. A. A Synthetic DNA Walker for Molecular Transport. *J. Am. Chem. Soc.* **2004**, *126*, 10834–10835.

(13) Wickham, S. F.; Bath, J.; Katsuda, Y.; Endo, M.; Hidaka, K.; Sugiyama, H.; Turberfield, A. J. A DNA-Based Molecular Motor That Can Navigate a Network of Tracks. *Nat. Nanotechnol.* **2012**, *7*, 169–173.

(14) Franco, E.; Friedrichs, E.; Kim, J.; Jungmann, R.; Murray, R.; Winfree, E.; Simmel, F. C. Timing Molecular Motion and Production with a Synthetic Transcriptional Clock. *Proc. Natl. Acad. Sci. U. S. A.* **2011**, *108*, E784–E793.

(15) Zhang, D. Y.; Seelig, G. Dynamic DNA Nanotechnology Using Strand-Displacement Reactions. *Nat. Chem.* **2011**, *3*, 103–113.

(16) Kapanidis, A. N.; Strick, T. Biology, One Molecule at a Time. *Trends Biochem. Sci.* **2009**, *34*, 234–243.

(17) Joo, C.; Balci, H.; Ishitsuka, Y.; Buranachai, C.; Ha, T. Advances in Single-Molecule Fluorescence Methods for Molecular Biology. *Annu. Rev. Biochem.* **2008**, *77*, 51–76.

(18) Muller, B. K.; Reuter, A.; Simmel, F. C.; Lamb, D. C. Single-Pair FRET Characterization of DNA Tweezers. *Nano Lett.* **2006**, *6*, 2814–2820.

(19) Goodman, R. P.; Heilemann, M.; Doose, S.; Erben, C. M.; Kapanidis, A. N.; Turberfield, A. J. Reconfigurable, Braced, Three-Dimensional DNA Nanostructures. *Nat. Nanotechnol.* **2008**, *3*, 93–96.

(20) Gietl, A.; Holzmeister, P.; Grohmann, D.; Tinnefeld, P. DNA Origami as Biocompatible Surface to Match Single-Molecule and Ensemble Experiments. *Nucleic Acids Res.* **2012**, *40*, e110.

(21) Stein, I. H.; Schuller, V.; Bohm, P.; Tinnefeld, P.; Liedl, T. Single-Molecule FRET Ruler Based on Rigid DNA Origami Blocks. *ChemPhysChem* **2011**, *12*, 689–695.

(22) Stein, I. H.; Steinhauer, C.; Tinnefeld, P. Single-Molecule Four-Color FRET Visualizes Energy-Transfer Paths on DNA Origami. *J. Am. Chem. Soc.* **2011**, *133*, 4193–4195.

(23) Tomov, T. E.; Tsukanov, R.; Masoud, R.; Liber, M.; Plavner, N.; Nir, E. Disentangling Subpopulations in Single-Molecule FRET and ALEX Experiments with Photon Distribution Analysis. *Biophys. J.* **2012**, *102*, 1163–1173.

(24) Masoud, R.; Tsukanov, R.; Tomov, T. E.; Plavner, N.; Liber, M.; Nir, E. Studying the Structural Dynamics of Bipedal DNA Motors with Single-Molecule Fluorescence Spectroscopy. *ACS Nano* **2012**, *6*, 6272–6283.

(25) Tomov, T. E.; Tsukanov, R.; Liber, M.; Masoud, R.; Plavner, N.; Nir, E. Rational Design of DNA Motors: Fuel Optimization through Single-Molecule Fluorescence. *J. Am. Chem. Soc.* **2013**, *135*, 11935–11941.

(26) Tsukanov, R.; Tomov, T. E.; Masoud, R.; Drory, H.; Plavner, N.; Liber, M.; Nir, E. Detailed Study of DNA Hairpin Dynamics Using

Single-Molecule Fluorescence Assisted by DNA Origami. *J. Phys. Chem. B* **2013**, *117*, 11932−11942.
(27) Tsukanov, R.; Tomov, T. E.; Berger, Y.; Liber, M.; Nir, E. Conformational Dynamics of DNA Hairpins at Millisecond Resolution Obtained from Analysis of Single-Molecule FRET Histograms. *J. Phys. Chem. B* **2013**, *117*, 16105−16109.
(28) Lund, K.; Manzo, A. J.; Dabby, N.; Michelotti, N.; Johnson-Buck, A.; Nangreave, J.; Taylor, S.; Pei, R. J.; Stojanovic, M. N.; Walter, N. G.; Winfree, E.; Yan, H. Molecular Robots Guided by Prescriptive Landscapes. *Nature* **2010**, *465*, 206−210.
(29) Steinhauer, C.; Jungmann, R.; Sobey, T. L.; Simmel, F. C.; Tinnefeld, P. DNA Origami as a Nanoscopic Ruler for Super-Resolution Microscopy. *Angew. Chem., Int. Ed.* **2009**, *48*, 8870−8873.
(30) Jungmann, R.; Steinhauer, C.; Scheible, M.; Kuzyk, A.; Tinnefeld, P.; Simmel, F. C. Single-Molecule Kinetics and Super-Resolution Microscopy by Fluorescence Imaging of Transient Binding on DNA Origami. *Nano Lett.* **2010**, *10*, 4756−4761.
(31) Johnson-Buck, A.; Nangreave, J.; Kim, D. N.; Bathe, M.; Yan, H.; Walter, N. G. Super-Resolution Fingerprinting Detects Chemical Reactions and Idiosyncrasies of Single DNA Pegboards. *Nano Lett.* **2013**, *13*, 728−733.
(32) Acuna, G. P.; Bucher, M.; Stein, I. H.; Steinhauer, C.; Kuzyk, A.; Holzmeister, P.; Schreiber, R.; Moroz, A.; Stefani, F. D.; Liedl, T.; Simmel, F. C.; Tinnefeld, P. Distance Dependence of Single-Fluorophore Quenching by Gold Nanoparticles Studied on DNA Origami. *ACS Nano* **2012**, *6*, 3189−3195.
(33) Johnson-Buck, A.; Nangreave, J.; Jiang, S.; Yan, H.; Walter, N. G. Multifactorial Modulation of Binding and Dissociation Kinetics on Two-Dimensional DNA Nanostructures. *Nano Lett.* **2013**, *13*, 2754−2759.
(34) Acuna, G. P.; Möller, F. M.; Holzmeister, P.; Beater, S.; Lalkens, B.; Tinnefeld, P. Fluorescence Enhancement at Docking Sites of DNA-Directed Self-Assembled Nanoantennas. *Science* **2012**, *338*, 506−510.
(35) Scheible, M. B.; Pardatscher, G.; Kuzyk, A.; Simmel, F. C. Single Molecule Characterization of DNA Binding and Strand Displacement Reactions on Lithographic DNA Origami Microarrays. *Nano Lett.* **2014**, *14*, 1627−1633.
(36) Jungmann, R.; Avendano, M. S.; Woehrstein, J. B.; Dai, M.; Shih, W. M.; Yin, P. Multiplexed 3d Cellular Super-Resolution Imaging with DNA-Paint and Exchange-Paint. *Nat. Methods* **2014**, *11*, 313−318.
(37) Sisamakis, E.; Valeri, A.; Kalinin, S.; Rothwell, P. J.; Seidel, C. A. Accurate Single-Molecule FRET Studies Using Multiparameter Fluorescence Detection. *Methods Enzymol.* **2010**, *475*, 455−514.
(38) Roy, R.; Hohng, S.; Ha, T. A Practical Guide to Single-Molecule FRET. *Nat. Methods* **2008**, *5*, 507−516.
(39) Kruger, A. C.; Hildebrandt, L. L.; Kragh, S. L.; Birkedal, V. In *Laboratory Methods in Cell Biology: Imaging*; Conn, P. M., Ed.; Elsevier Academic Press Inc: San Diego, CA, 2012; Vol. *113*, pp 1−37.
(40) Walter, N. G.; Huang, C. Y.; Manzo, A. J.; Sobhy, M. A. Do-It-Yourself Guide: How to Use the Modern Single-Molecule Toolkit. *Nat. Methods* **2008**, *5*, 475−489.
(41) Zhao, R.; Rueda, D. RNA Folding Dynamics by Single-Molecule Fluorescence Resonance Energy Transfer. *Methods* **2009**, *49*, 112−117.
(42) Schuler, B.; Hofmann, H. Single-Molecule Spectroscopy of Protein Folding Dynamics-Expanding Scope and Timescales. *Curr. Opin. Chem. Biol.* **2013**, *23*, 36−47.
(43) Kapanidis, A. N.; Lee, N. K.; Laurence, T. A.; Doose, S.; Margeat, E.; Weiss, S. Fluorescence-Aided Molecule Sorting: Analysis of Structure and Interactions by Alternating-Laser Excitation of Single Molecules. *Proc. Natl. Acad. Sci. U. S. A.* **2004**, *101*, 8936−8941.
(44) Nir, E.; Michalet, X.; Hamadani, K. M.; Laurence, T. A.; Neuhauser, D.; Kovchegov, Y.; Weiss, S. Shot-Noise Limited Single-Molecule FRET Histograms: Comparison between Theory and Experiments. *J. Phys. Chem. B* **2006**, *110*, 22103−22124.
(45) Kudryavtsev, V.; Sikor, M.; Kalinin, S.; Mokranjac, D.; Seidel, C. A. M.; Lamb, D. C. Combining MFD and PIE for Accurate Single-Pair Forster Resonance Energy Transfer Measurements. *ChemPhysChem* **2012**, *13*, 1060−1078.
(46) Axelrod, D. Total Internal Reflection Fluorescence Microscopy in Cell Biology. *Methods Enzymol.* **2003**, *361*, 1−33.
(47) Michelotti, N.; de Silva, C.; Johnson-Buck, A. E.; Manzo, A. J.; Walter, N. G. A Bird's Eye View Tracking Slow Nanometer-Scale Movements of Single Molecular Nano-Assemblies. *Methods Enzymol.* **2010**, *475*, 121−148.
(48) Jungmann, R.; Scheible, M.; Simmel, F. C. Nanoscale Imaging in DNA Nanotechnology. *Wiley Interdiscip. Rev.: Nanomed. Nanobiotechnol.* **2012**, *4*, 66−81.
(49) Birkedal, V.; Dong, M.; Golas, M. M.; Sander, B.; Andersen, E. S.; Gothelf, K. V.; Besenbacher, F.; Kjems, J. Single Molecule Microscopy Methods for the Study of DNA Origami Structures. *Microsc. Res. Technol.* **2011**, *74*, 688−698.
(50) Rajendran, A.; Endo, M.; Sugiyama, H. Single-Molecule Analysis Using DNA Origami. *Angew. Chem., Int. Ed.* **2012**, *51*, 874−890.
(51) Rueda, D.; Walter, N. G. Single Molecule Fluorescence Control for Nanotechnology. *J. Nanosci. Nanotechnol.* **2005**, *5*, 1990−2000.
(52) Preus, S.; Wilhelmsson, L. M. Advances in Quantitative FRET-Based Methods for Studying Nucleic Acids. *ChemBioChem* **2012**, *13*, 1990−2001.
(53) Ha, T.; Tinnefeld, P. Photophysics of Fluorescent Probes for Single-Molecule Biophysics and Super-Resolution Imaging. *Annu. Rev. Phys. Chem.* **2012**, *63*, 595−617.
(54) Kalinin, S.; Felekyan, S.; Valeri, A.; Seidel, C. A. M. Characterizing Multiple Molecular States in Single-Molecule Multiparameter Fluorescence Detection by Probability Distribution Analysis. *J. Phys. Chem. B* **2008**, *112*, 8361−8374.
(55) Santoso, Y.; Torella, J. P.; Kapanidis, A. N. Characterizing Single-Molecule FRET Dynamics with Probability Distribution Analysis. *ChemPhysChem* **2010**, *11*, 2209−2219.
(56) Antonik, M.; Felekyan, S.; Gaiduk, A.; Seidel, C. A. M. Separating Structural Heterogeneities from Stochastic Variations in Fluorescence Resonance Energy Transfer Distributions Via Photon Distribution Analysis. *J. Phys. Chem. B* **2006**, *110*, 6970−6978.
(57) Chung, H. S.; Gopich, I. V.; McHale, K.; Cellmer, T.; Louis, J. M.; Eaton, W. A. Extracting Rate Coefficients from Single-Molecule Photon Trajectories and FRET Efficiency Histograms for a Fast-Folding Protein. *J. Phys. Chem. A* **2011**, *115*, 3642−3656.